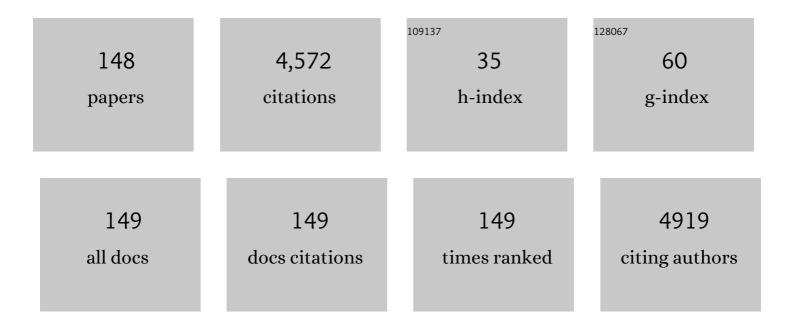
List of Publications by Year in descending order

Source: https://exaly.com/author-pdf/4047534/publications.pdf Version: 2024-02-01



#	Article	IF	CITATIONS
1	MOFs-derived porous carbon/NiFeP hierarchical flower-like nanoarchitectures for efficient overall water splitting. Journal Physics D: Applied Physics, 2022, 55, 055502.	1.3	0
2	A host–guest self-assembly strategy to enhance π-electron densities in ultrathin porous carbon nitride nanocages toward highly efficient hydrogen evolution. Chemical Engineering Journal, 2022, 430, 132880.	6.6	33
3	Highly efficient tree search algorithm for irreducible site-occupancy configurations. Physical Review B, 2022, 105, .	1.1	6
4	Two-dimensional chromium phosphorus monolayer based gas sensors to detect NOx: A first-principles study. Results in Physics, 2022, 32, 105100.	2.0	10
5	Symmetry-Breaking-Induced Multifunctionalities of Two-Dimensional Chromium-Based Materials for Nanoelectronics and Clean Energy Conversion. Physical Review Applied, 2022, 18, .	1.5	18
6	A two-dimensional MoS2/SnS heterostructure for promising photocatalytic performance: First-principles investigations. Physica E: Low-Dimensional Systems and Nanostructures, 2021, 126, 114453.	1.3	17
7	Strain and interfacial engineering to accelerate hydrogen evolution reaction of two-dimensional phosphorus carbide*. Chinese Physics B, 2021, 30, 027101.	0.7	2
8	Co-Cu-P nanosheet-based open architecture for high-performance oxygen evolution reaction. Applied Physics A: Materials Science and Processing, 2021, 127, 1.	1.1	7
9	Supersaturation-triggered synthesis of 2D/1D phosphide heterostructures as multi-functional catalysts for water splitting. Applied Physics Letters, 2021, 118, .	1.5	10
10	Highâ€Throughput Oneâ€Photon Excitation Pathway in 0D/3D Heterojunctions for Visibleâ€Light Driven Hydrogen Evolution. Advanced Functional Materials, 2021, 31, 2100816.	7.8	92
11	Oneâ€Photon Excitation Pathway: Highâ€Throughput Oneâ€Photon Excitation Pathway in 0D/3D Heterojunctions for Visible‣ight Driven Hydrogen Evolution (Adv. Funct. Mater. 18/2021). Advanced Functional Materials, 2021, 31, 2170125.	7.8	1
12	Construction of ZnxCd1â [~] 'xS/CeO2 composites for enhanced photocatalytic activity and stability by chemical precipitation method. Modern Physics Letters B, 2021, 35, 2150333.	1.0	0
13	Novel urchin-like CoNiP as advanced pH-universal electrocatalysts toward hydrogen evolution reaction. Journal Physics D: Applied Physics, 2021, 54, 365502.	1.3	5
14	Amorphous B-doped graphitic carbon nitride quantum dots with high photoluminescence quantum yield of near 90% and their sensitive detection of Fe2+/Cd2+. Science China Materials, 2021, 64, 3037-3050.	3.5	17
15	2D Amorphous CoO Incorporated g ₃ N ₄ Nanotubes for Improved Photocatalytic Performance. Physica Status Solidi - Rapid Research Letters, 2021, 15, 2100254.	1.2	6
16	High-throughput computational design for 2D van der Waals functional heterostructures: Fragility of Anderson's rule and beyond. Applied Physics Letters, 2021, 119, .	1.5	24
17	Acid-induced topological morphology modulation of graphitic carbon nitride homojunctions as advanced metal-free catalysts for OER and pollutant degradation. Journal of Materials Science and Technology, 2021, 86, 210-218.	5.6	18
18	Generalized Synthetic Strategy for Amorphous Transition Metal Oxidesâ€Based 2D Heterojunctions with Superb Photocatalytic Hydrogen and Oxygen Evolution. Advanced Functional Materials, 2021, 31, 2009230.	7.8	97

#	ARTICLE	IF	CITATIONS
19	Dipole Engineering of Two-Dimensional van der Waals Heterostructures for Enhanced Power-Conversion Efficiency: The Case of Janus <mml:math xmlns:mml="http://www.w3.org/1998/Math/MathML" display="inline" overflow="scroll"><mml:msub><mml:mi>Ga</mml:mi><mml:mn>2</mml:mn></mml:msub><mml:mrow><mml:< td=""><td>1.5 mi>Se<td>39 ıml:mi><mm< td=""></mm<></td></td></mml:<></mml:mrow></mml:math 	1.5 mi>Se <td>39 ıml:mi><mm< td=""></mm<></td>	39 ıml:mi> <mm< td=""></mm<>
20	In situ construction of hierarchical graphitic carbon nitride homojunction as robust bifunctional photoelectrocatalyst for overall water splitting. Journal of Chemical Technology and Biotechnology, 2020, 95, 758-769.	1.6	6
21	Interfacial charge modulation: carbon quantum dot implanted carbon nitride double-deck nanoframes for robust visible-light photocatalytic tetracycline degradation. Nanoscale, 2020, 12, 3135-3145.	2.8	45
22	Ultrahigh Sensitivity and Selectivity of Pentagonal SiC ₂ Monolayer Gas Sensors: The Synergistic Effect of Composition and Structural Topology. Physica Status Solidi (B): Basic Research, 2020, 257, 1900445.	0.7	11
23	Algorithm for generating irreducible site-occupancy configurations. Physical Review B, 2020, 102, .	1.1	16
24	NiFe ₂ O ₄ /NiFeP Heterostructure Grown on Nickel Foam as an Efficient Electrocatalyst for Water Oxidation. ChemElectroChem, 2020, 7, 4047-4054.	1.7	15
25	Ultra-thin tubular graphitic carbon Nitride-Carbon Dot lateral heterostructures: One-Step synthesis and highly efficient catalytic hydrogen generation. Chemical Engineering Journal, 2020, 397, 125470.	6.6	72
26	Hierarchical Self-assembly of Well-Defined Louver-Like P-Doped Carbon Nitride Nanowire Arrays with Highly Efficient Hydrogen Evolution. Nano-Micro Letters, 2020, 12, 52.	14.4	45
27	Type-II/type-II band alignment to boost spatial charge separation: a case study of g-C ₃ N ₄ quantum dots/a-TiO ₂ /r-TiO ₂ for highly efficient photocatalytic hydrogen and oxygen evolution. Nanoscale, 2020, 12, 6037-6046.	2.8	79
28	From monolayer to lateral heterostructure of functionalized phosphorus carbide: Evolution of electronic properties. Physica E: Low-Dimensional Systems and Nanostructures, 2020, 118, 113962.	1.3	6
29	A design rule for two-dimensional van der Waals heterostructures with unconventional band alignments. Physical Chemistry Chemical Physics, 2020, 22, 3037-3047.	1.3	19
30	Organic Small Molecule Activates Transition Metal Foam for Efficient Oxygen Evolution Reaction. Advanced Materials, 2020, 32, e1906015.	11.1	56
31	Strain and Electric Field Controllable Schottky Barriers and Contact Types in Graphene-MoTe2 van der Waals Heterostructure. Nanoscale Research Letters, 2020, 15, 180.	3.1	15
32	Strategy to boost catalytic activity of polymeric carbon nitride: synergistic effect of controllable <i>in situ</i> surface engineering and morphology. Nanoscale, 2019, 11, 16393-16405.	2.8	45
33	Monolayer Phosphorene–Carbon Nanotube Heterostructures for Photocatalysis: Analysis by Density Functional Theory. Nanoscale Research Letters, 2019, 14, 233.	3.1	10
34	Steering charge kinetics boost the photocatalytic activity of graphitic carbon nitride: heteroatom-mediated spatial charge separation and transfer. Journal Physics D: Applied Physics, 2019, 53, 015502.	1.3	28
35	Chlorine doped graphitic carbon nitride nanorings as an efficient photoresponsive catalyst for water oxidation and organic decomposition. Journal of Materials Science and Technology, 2019, 35, 2288-2296.	5.6	61
36	0D/2D Z-scheme heterojunctions of g-C3N4 quantum dots/ZnO nanosheets as a highly efficient visible-light photocatalyst. Advanced Powder Technology, 2019, 30, 1576-1583.	2.0	40

#	Article	IF	CITATIONS
37	Tunable Schottky barrier in van der Waals heterostructures of graphene and hydrogenated phosphorus carbide monolayer: first-principles calculations. Journal Physics D: Applied Physics, 2019, 52, 305104.	1.3	18
38	Dimensional transformation and morphological control of graphitic carbon nitride from water-based supramolecular assembly for photocatalytic hydrogen evolution: from 3D to 2D and 1D nanostructures. Applied Catalysis B: Environmental, 2019, 254, 321-328.	10.8	134
39	Doping-induced enhancement of crystallinity in polymeric carbon nitride nanosheets to improve their visible-light photocatalytic activity. Nanoscale, 2019, 11, 6876-6885.	2.8	128
40	Doping-Induced Hydrogen-Bond Engineering in Polymeric Carbon Nitride To Significantly Boost the Photocatalytic H ₂ Evolution Performance. ACS Applied Materials & Interfaces, 2019, 11, 17341-17349.	4.0	71
41	Hollow BCN microrods with hierarchical multichannel structure as a multifunctional material: Synergistic effects of structural topology and composition. Carbon, 2019, 148, 231-240.	5.4	29
42	Protonated supramolecular complex-induced porous graphitic carbon nitride nanosheets as bifunctional catalyst for water oxidation and organic pollutant degradation. Journal of Materials Science, 2019, 54, 7637-7650.	1.7	16
43	Electrostatic Potential Anomaly in 2D Janus Transition Metal Dichalcogenides. Annalen Der Physik, 2019, 531, 1900369.	0.9	13
44	Penta-Graphene as a Potential Gas Sensor for NOx Detection. Nanoscale Research Letters, 2019, 14, 306.	3.1	52
45	Hydroxy-carbonate-assisted synthesis of high porous graphitic carbon nitride with broken of hydrogen bonds as a highly efficient visible-light-driven photocatalyst. Journal Physics D: Applied Physics, 2019, 52, 105502.	1.3	32
46	Twoâ€Dimensional GaX/SnS ₂ (<i>X</i> = S, Se) van der Waals Heterostructures for Photovoltaic Application: Heteroatom Doping Strategy to Boost Power Conversion Efficiency. Physica Status Solidi - Rapid Research Letters, 2019, 13, 1800565.	1.2	35
47	Isotype heterojunction g-C ₃ N ₄ /g-C ₃ N ₄ anosheets as 2D support to highly dispersed 0D metal oxide nanoparticles: Generalized self-assembly and its high photocatalytic activity. Journal Physics D: Applied Physics, 2019, 52, 025501.	1.3	46
48	Porous graphitic carbon nitride with lamellar structure: Facile synthesis via in-site supramolecular self-assembly in alkaline solutions and superior photocatalytic activity. Advanced Powder Technology, 2019, 30, 120-125.	2.0	8
49	Insights Into Interfacial Interaction and Its Influence on the Electronic and Optical Properties of Twoâ€Dimensional WS ₂ /TX ₂ CO ₂ (TX = Ti, Zr) van der Waals Heterostructures. Physica Status Solidi (B): Basic Research, 2019, 256, 1800377.	0.7	2
50	Self-assembled hierarchical carbon/g-C ₃ N ₄ composite with high photocatalytic activity. Journal Physics D: Applied Physics, 2018, 51, 135501.	1.3	12
51	Interfacial Interaction between Boron Cluster and Metal Oxide Surface and Its Effects: A Case Study of B ₂₀ /Ag ₃ PO ₄ van der Waals Heterostructure. Journal of Physical Chemistry C, 2018, 122, 6151-6158.	1.5	7
52	Facile <i>in situ</i> synthesis of wurtzite ZnS/ZnO core/shell heterostructure with highly efficient visible-light photocatalytic activity and photostability. Journal Physics D: Applied Physics, 2018, 51, 075501.	1.3	36
53	Facile synthesis and superior photocatalytic and electrocatalytic performances of porous B-doped g-C3N4 nanosheets. Journal of Materials Science and Technology, 2018, 34, 2515-2520.	5.6	87
54	Interfacial Interactions in Monolayer and Few‣ayer SnS/CH ₃ NH ₃ PbI ₃ Perovskite van der Waals Heterostructures and Their Effects on Electronic and Optical Properties. ChemPhysChem. 2018, 19, 291-299.	1.0	12

#	Article	IF	CITATIONS
55	Theory-Driven Heterojunction Photocatalyst Design with Continuously Adjustable Band Gap Materials. Journal of Physical Chemistry C, 2018, 122, 28065-28074.	1.5	20
56	Facile <i>in situ</i> construction of mediator-free direct Z-scheme g-C ₃ N ₄ /CeO ₂ heterojunctions with highly efficient photocatalytic activity. Journal Physics D: Applied Physics, 2018, 51, 275302.	1.3	110
5 7	Dispersive and covalent interactions in all-carbon heterostructures consisting of penta-graphene and fullerene: topological effect. Journal Physics D: Applied Physics, 2018, 51, 305301.	1.3	12
58	In-situ construction of 2D direct Z-scheme g-C3N4/g-C3N4 homojunction with high photocatalytic activity. Journal of Materials Science, 2018, 53, 15882-15894.	1.7	52
59	Substrate-induced magnetism and topological phase transition in silicene. Nanoscale, 2018, 10, 14667-14677.	2.8	10
60	Simultaneous dispersive and covalent monolayer MoS2/TiO2 cluster heterostructures: Insights into their enhanced photocatalytic activity. Superlattices and Microstructures, 2018, 121, 64-74.	1.4	0
61	Mesoporous g-C3N4 Nanosheets: Synthesis, Superior Adsorption Capacity and Photocatalytic Activity. Journal of Nanoscience and Nanotechnology, 2018, 18, 5502-5510.	0.9	19
62	Tuning the near-gap electronic structure of Cu2O by anion–cation co-doping for enhanced solar energy conversion. Modern Physics Letters B, 2017, 31, 1650429.	1.0	4
63	Electronic and optical properties of Cr-, B-doped, and (Cr, B)-codoped SrTiO ₃ . International Journal of Modern Physics B, 2017, 31, 1750064.	1.0	2
64	Simultaneous covalent and noncovalent carbon nanotube/Ag ₃ PO ₄ hybrids: new insights into the origin of enhanced visible light photocatalytic performance. Physical Chemistry Chemical Physics, 2017, 19, 7955-7963.	1.3	13
65	Construction of g-C 3 N 4 /CeO 2 /ZnO ternary photocatalysts with enhanced photocatalytic performance. Journal of Physics and Chemistry of Solids, 2017, 106, 1-9.	1.9	116
66	Hybrid TiO ₂ /graphene derivatives nanocomposites: is functionalized graphene better than pristine graphene for enhanced photocatalytic activity?. Catalysis Science and Technology, 2017, 7, 1423-1432.	2.1	20
67	Origin of enhanced visible-light photocatalytic activity of transition-metal (Fe, Cr and Co)-doped CeO2: effect of 3d orbital splitting. Applied Physics A: Materials Science and Processing, 2017, 123, 1.	1.1	37
68	Two-Dimensional MoS ₂ -Graphene-Based Multilayer van der Waals Heterostructures: Enhanced Charge Transfer and Optical Absorption, and Electric-Field Tunable Dirac Point and Band Gap. Chemistry of Materials, 2017, 29, 5504-5512.	3.2	131
69	Interfacial interaction in monolayer transition metal dichalcogenide/metal oxide heterostructures and its effects on electronic and optical properties: The case of MX ₂ /CeO ₂ . Applied Physics Express, 2017, 10, 011201.	1.1	11
70	Noncovalent Functionalization of Monolayer MoS ₂ with Carbon Nanotubes: Tuning Electronic Structure and Photocatalytic Activity. Journal of Physical Chemistry C, 2017, 121, 21921-21929.	1.5	23
71	Novel <i>β</i> -C ₃ N ₄ /CuO nanoflakes: facile synthesis and unique photocatalytic performance. Journal Physics D: Applied Physics, 2017, 50, 355501.	1.3	10
72	The mechanism of enhanced photocatalytic activity of SnO 2 through fullerene modification. Current Applied Physics, 2017, 17, 1547-1556.	1.1	14

#	Article	IF	CITATIONS
73	Facile one-step in-situ synthesis of type-II CeO2/CeF3 composite with tunable morphology and photocatalytic activity. Ceramics International, 2016, 42, 16374-16381.	2.3	15
74	Dual role of monolayer MoS2 in enhanced photocatalytic performance of hybrid MoS2/SnO2 nanocomposite. Journal of Applied Physics, 2016, 119, .	1.1	57
75	Insights into enhanced visible-light photocatalytic activity of C ₆₀ modified g-C ₃ N ₄ hybrids: the role of nitrogen. Physical Chemistry Chemical Physics, 2016, 18, 33094-33102.	1.3	31
76	Tunable synthesis of various ZnO architectural structures with enhanced photocatalytic activities. Materials Letters, 2016, 175, 68-71.	1.3	23
77	Electronic properties and photoactivity of monolayer MoS ₂ /fullerene van der Waals heterostructures. RSC Advances, 2016, 6, 43228-43236.	1.7	28
78	A facile and rapid route for synthesis of g-C ₃ N ₄ nanosheets with high adsorption capacity and photocatalytic activity. RSC Advances, 2016, 6, 86688-86694.	1.7	81
79	Mechanism of enhanced photocatalytic activities on tungsten trioxide doped with sulfur: Dopant-type effects. Modern Physics Letters B, 2016, 30, 1650340.	1.0	6
80	Non-covalent functionalization of WS ₂ monolayer with small fullerenes: tuning electronic properties and photoactivity. Dalton Transactions, 2016, 45, 13383-13391.	1.6	22
81	Dual functions of 2D WS ₂ and MoS ₂ –WS ₂ monolayers coupled with a Ag ₃ PO ₄ photocatalyst. Semiconductor Science and Technology, 2016, 31, 095013.	1.0	8
82	Enhanced photocatalytic activity of hexagonal flake-like Bi ₂ S ₃ / ZnS composites with a large percentage of reactive facets. Journal Physics D: Applied Physics, 2016, 49, 305105.	1.3	17
83	Dramatically Enhanced Visible Light Response of Monolayer ZrS2 via Non-covalent Modification by Double-Ring Tubular B20 Cluster. Nanoscale Research Letters, 2016, 11, 495.	3.1	25
84	Facile route to fabricate carbon-doped TiO2 nanoparticles and its mechanism of enhanced visible light photocatalytic activity. Applied Physics A: Materials Science and Processing, 2016, 122, 1.	1.1	16
85	Tuning near-gap electronic structure, interface charge transfer and visible light response of hybrid doped graphene and Ag3PO4 composite: Dopant effects. Scientific Reports, 2016, 6, 22267.	1.6	24
86	Facile ion-exchange synthesis of mesoporous Bi 2 S 3 /ZnS nanoplate with high adsorption capability and photocatalytic activity. Journal of Colloid and Interface Science, 2016, 464, 103-109.	5.0	35
87	Enhanced photocatalytic performance of an Ag ₃ PO ₄ photocatalyst via fullerene modification: first-principles study. Physical Chemistry Chemical Physics, 2016, 18, 2878-2886.	1.3	22
88	Origin of enhanced photocatalytic activity of F-doped CeO2 nanocubes. Applied Surface Science, 2016, 370, 427-432.	3.1	50
89	Insights into enhanced visible-light photocatalytic activity of CeO 2 doped with nonmetal impurity from the first principles. Materials Science in Semiconductor Processing, 2016, 41, 200-208.	1.9	44
90	Insights into Enhanced Visible-Light Photocatalytic Hydrogen Evolution of g-C ₃ N ₄ and Highly Reduced Graphene Oxide Composite: The Role of Oxygen. Chemistry of Materials, 2015, 27, 1612-1621.	3.2	252

#	Article	IF	CITATIONS
91	Origin of photocatalytic activity of nitrogen-doped germanium dioxide under visible light from first principles. Materials Science in Semiconductor Processing, 2015, 31, 517-524.	1.9	8
92	Half-metallic ferromagnetism in Fe-chain-embedded zigzag boron-nitride nanoribbons with line defect. Physica E: Low-Dimensional Systems and Nanostructures, 2015, 74, 431-437.	1.3	2
93	Electronic Structures and Photocatalytic Responses of SrTiO ₃ (100) Surface Interfaced with Graphene, Reduced Graphene Oxide, and Graphane: Surface Termination Effect. Journal of Physical Chemistry C, 2015, 119, 19095-19104.	1.5	32
94	Enhancement of photocatalytic activity of combustion-synthesized CeO2/C3N4 nanoparticles. Applied Physics A: Materials Science and Processing, 2015, 120, 1205-1209.	1.1	18
95	Mass production of ZnxCd1â^'xS nanoparticles with enhanced visible light photocatalytic activity. Materials Letters, 2015, 158, 432-435.	1.3	11
96	A novel photocatalyst CeF ₃ : facile fabrication and photocatalytic performance. RSC Advances, 2015, 5, 95171-95177.	1.7	19
97	Morphology-controlled SnS2 nanostructures synthesized by refluxing method with high photocatalytic activity. Materials Letters, 2015, 161, 480-483.	1.3	18
98	Enhanced photocatalytic activity and stability of Zn Cd1â^'S/TiO2 nanocomposites synthesized by chemical bath deposition. Materials Letters, 2015, 142, 133-136.	1.3	15
99	Band structure engineering of monolayer MoS ₂ : a charge compensated codoping strategy. RSC Advances, 2015, 5, 7944-7952.	1.7	26
100	Reversal of thermal rectification in one-dimensional nonlinear composite system. Chinese Physics B, 2014, 23, 114401.	0.7	2
101	THE ELECTRONIC AND OPTICAL PROPERTIES OF X-DOPED SrTiO ₃ (X = Rh, Pd,) Tj ETC	2q110.78	4314 rgBT /O
102	Annealing Effects on Photocatalytic Activity of Zn0.2Cd0.8S Films Prepared by Chemical Bath Deposition. Journal of Nanomaterials, 2014, 2014, 1-6.	1.5	5
103	The enhanced photocatalytic activity of Ti3+ self-doped TiO2 by a reduction method. Materials Letters, 2014, 122, 33-36.	1.3	32
104	Novel 3D flower-like Ag3PO4 microspheres with highly enhanced visible light photocatalytic activity. Materials Letters, 2014, 116, 209-211.	1.3	45
105	Novel Ag ₃ PO ₄ /CeO ₂ composite with high efficiency and stability for photocatalytic applications. Journal of Materials Chemistry A, 2014, 2, 1750-1756.	5.2	251
106	Band engineering of ZnS by codoping for visible-light photocatalysis. Applied Physics A: Materials Science and Processing, 2014, 116, 741-750.	1.1	32
107	Band gap engineering by lanthanide doping in the photocatalyst LaOF: First-principles study. International Journal of Modern Physics B, 2014, 28, 1450069.	1.0	6
108	Interfacial Interactions of Semiconductor with Graphene and Reduced Graphene Oxide: CeO ₂ as a Case Study. ACS Applied Materials & Interfaces, 2014, 6, 20350-20357.	4.0	71

#	Article	IF	CITATIONS
109	Native vacancy defects in bismuth sulfide. International Journal of Modern Physics B, 2014, 28, 1450150.	1.0	15
110	Electrospinning preparation of p-type NiO/n-type CeO 2 heterojunctions with enhanced photocatalytic activity. Materials Letters, 2014, 133, 109-112.	1.3	37
111	Facile shape-controllable synthesis of Ag 3 PO 4 photocatalysts. Materials Letters, 2014, 133, 139-142.	1.3	33
112	Theoretical insight into the electronic and photocatalytic properties of Cu2O from a hybrid density functional theory. Materials Science in Semiconductor Processing, 2014, 23, 34-41.	1.9	16
113	Mechanism of Superior Visible-Light Photocatalytic Activity and Stability of Hybrid Ag ₃ PO ₄ /Graphene Nanocomposite. Journal of Physical Chemistry C, 2014, 118, 12972-12979.	1.5	78
114	Band-Gap Widening of Nitrogen-Doped Cu ₂ O: New Insights from First-Principles Calculations. Science of Advanced Materials, 2014, 6, 1221-1227.	0.1	10
115	Luminescent and photocatalytic properties of hollow SnO2 nanospheres. Materials Science and Engineering B: Solid-State Materials for Advanced Technology, 2013, 178, 725-729.	1.7	16
116	Efficient ultraviolet emission of ZnS nanospheres: Co doping enhancement. Materials Letters, 2013, 100, 237-240.	1.3	24
117	<pre><mml:math <br="" xmins:mml="http://www.w3.org/1998/Math/Math/ML">id="M1"><mml:mrow><mml:msub><mml:mrow><mml:mtext>Ag</mml:mtext></mml:mrow><mml:mrow><mml:mrow><mml:mrow><mml:mtext>PO</mml:mtext>mathvariant="bold">3</mml:mrow></mml:mrow></mml:mrow></mml:msub><mml:msub><mml:mrow><mml:mtext>PO</mml:mtext>mathvariant="bold">4</mml:mrow></mml:msub></mml:mrow></mml:math>Semiconductor</pre>	mr ውነ ള > < m	ml 38 n
118	Coupling effect of La doping and porphyrin sensitization on photocatalytic activity of nanocrystalline TiO2. Materials Letters, 2013, 108, 37-40.	1.3	32
119	Enhanced visible-light photoactivity of La-doped ZnS thin films. Applied Physics A: Materials Science and Processing, 2012, 108, 895-900.	1.1	34
120	Orientation-controlled synthesis and magnetism of single crystalline Co nanowires. Journal of Magnetism and Magnetic Materials, 2012, 324, 4043-4047.	1.0	10
121	Effects of contact shape on ballistic phonon transport in semiconductor nanowires. Current Applied Physics, 2012, 12, 437-442.	1.1	Ο
122	Visible-light absorption and photocatalytic activity of Cr-doped TiO2 nanocrystal films. Advanced Powder Technology, 2012, 23, 8-12.	2.0	198
123	Annealing effects on photocatalytic activity of ZnS films prepared by chemical bath deposition. Materials Letters, 2012, 75, 221-224.	1.3	33
124	Size-controllable synthesis and enhanced photocatalytic activity of porous ZnS nanospheres. Materials Letters, 2012, 83, 104-107.	1.3	46
125	Effect of Gaussian acoustic nanocavities in a narrow constriction on ballistic phonon transmission. Applied Physics A: Materials Science and Processing, 2011, 104, 635-642.	1.1	2
126	Ballistic phonon transport through a Fibonacci array of acoustic nanocavities in a narrow constriction. Physics Letters, Section A: General, Atomic and Solid State Physics, 2011, 375, 2000-2006.	0.9	1

#	Article	IF	CITATIONS
127	Ballistic phonon transmission in quasiperiodic acoustic nanocavities. Journal of Applied Physics, 2011, 109, 084310.	1.1	3
128	Ballistic phonon transmission in a symmetric converging–diverging contact of a semiconductor nanowire. Journal Physics D: Applied Physics, 2011, 44, 105102.	1.3	2
129	Optical Characteristics of La-Doped ZnS Thin Films Prepared by Chemical Bath Deposition. Chinese Physics Letters, 2011, 28, 027806.	1.3	11
130	BALLISTIC PHONON TRANSPORT THROUGH GAUSSIAN ACOUSTIC NANOCAVITIES. Modern Physics Letters B, 2011, 25, 1631-1642.	1.0	4
131	Material properties dependence of ballistic phonon transmission through two coupled nanocavities. Journal of Applied Physics, 2009, 105, 124305.	1.1	10
132	INVESTIGATION OF BIAXIAL ELASTIC MODULUS AND CTE OF BaTiO3 FILMS. International Journal of Modern Physics B, 2009, 23, 4933-4941.	1.0	1
133	Selective transmission and enhanced thermal conductance of ballistic phonon by nanocavities embedded in a narrow constriction. Journal Physics D: Applied Physics, 2009, 42, 015101.	1.3	8
134	Magnetic properties of CoFeP films prepared by electroless deposition. Journal of Magnetism and Magnetic Materials, 2009, 321, 1177-1181.	1.0	17
135	Effects of Lanthanum on Magnetic Behavior and Hardness of Electroless Ni–Fe–P Deposits. International Journal of Materials Research, 2009, 100, 667-671.	0.1	1
136	Selective transport of ballistic phonon modes by an acoustic nanocavity in a Î ⁻ -shaped semiconductor nanowire. Journal of Applied Physics, 2008, 104, 054309.	1.1	10
137	Phonon-cavity-enhanced low-temperature thermal conductance of a semiconductor nanowire with narrow constrictions. Physical Review B, 2007, 75, .	1.1	24
138	The influence of Nd on the corrosion behavior of electroless-deposited Fe–P. International Journal of Materials Research, 2007, 98, 217-220.	0.1	4
139	Electrochemical study of electroless deposition of Fe–P alloys. Electrochimica Acta, 2006, 51, 4471-4476.	2.6	31
140	Preparation of amorphous rare-earth films of Ni–Re–P (Re=Ce, Nd) by electrodeposition from an aqueous bath. Surface and Coatings Technology, 2005, 192, 208-212.	2.2	18
141	The electrochemical behavior and surface structure of titanium electrodes modified by ion beams. Applied Surface Science, 2004, 236, 13-17.	3.1	3
142	The mechanical performance and anti-corrosion behavior of diamond-like carbon film. Diamond and Related Materials, 2003, 12, 1406-1410.	1.8	44
143	Combined effect of thickness and stress on ferroelectric behavior of thin BaTiO3 films. Journal of Applied Physics, 2003, 93, 2855-2860.	1.1	35
144	Study of Magnetic Properties of Ni–Fe–P and Ni–Fe–P–B Chemical Films. International Journal of Materials Research, 2002, 93, 298-302.	0.8	4

#	Article	IF	CITATIONS
145	Composition, structure and corrosion characteristics of Ni–Fe–P and Ni–Fe–P–B alloy deposits prepared by electroless plating. Surface and Coatings Technology, 2000, 126, 272-278.	2.2	44
146	Crystallization of Ni-Fe-P amorphous films prepared by electroless plating. , 2000, , .		0
147	Generalized Multidentate Ligand Chelatingâ€Grafting Strategy for Construction of Amorphous Metal Oxidesâ€Based Tripleâ€Layered Nanotubes. Physica Status Solidi (A) Applications and Materials Science, 0, , .	0.8	0
148	Dataâ€Ðriven Approach to Designing Twoâ€dimensional Van der Waals Heterostructures: Misjudgment of Band Alignment Type and its mechanism. Physica Status Solidi - Rapid Research Letters, 0, , .	1.2	2